SOFT X-RAY MEASUREMENTS ON THE REPUTE-1 REVERSED FIELD PINCH

N. ASAKURA*, Y. NAGAYAMA, S. SHINOHARA,
H. TOYAMA, K. MIYAMOTO
Department of Physics,
Faculty of Science,
University of Tokyo

N. INOUE
Department of Nuclear Engineering,
Faculty of Engineering,
University of Tokyo

Tokyo, Japan

ABSTRACT. Soft X-ray measurements have been made with surface barrier diode (SBD) arrays in the REPUTE-1 RFP device (R/a = 82/22 cm). Arrays of seven and eleven SBDs are arranged so that they view a minor cross-section of the plasma from the vertical and horizontal diagnostic ports, respectively. Applying the tomography technique to the soft X-ray data, a two-dimensional emissivity profile can be reconstructed. In the sustainment phase of the RFP discharge, the soft X-ray emissivity profile exhibits a periodic peaking and a subsequent large crash across the minor cross-section. The fluctuation period is in the range of 60–150 μs, whereas the duration of the large crash is always about 30 μs (corresponding to $\sim 100 \times \tau_A$, where τ_A is the Alfvén transit time). The soft X-ray emission is due to two modes: one is a dominantly m = 0 mode, which corresponds to the axisymmetric increase or decrease of the soft X-ray emissivity profile, and the other is an m = 1 mode. The toroidal correlation length of the m = 0 mode ranges from 20° to 80°, while the m = 1 mode has a high toroidal mode number. In the crash process, an m = 1 distortion of the emissivity profile, which indicates reconnection of the flux surfaces, can be observed. The magnetic fluctuations observed simultaneously are well correlated with the soft X-ray fluctuations. It is found that the soft X-ray fluctuations reflect the relaxation mechanism of the RFP plasma. This phenomenon is considered to be driven by global MHD activity.

1. INTRODUCTION

Recently, it has been found in numerous experiments that a reversed field pinch (RFP) plasma can be maintained for a longer period than the magnetic diffusion time ($\tau_R = \mu_0 a^2/\eta_0$, where μ_0 is the magnetic permeability, a is the plasma minor radius and η_0 is the plasma resistivity) [1–4] and that the toroidal magnetic flux is generated in the sustainment phase of an RFP discharge [5–7]. These phenomena are commonly regarded as a 'dynamo' effect, in analogy with an astrophysical process [8]. Experimental and numerical results indicate that these phenomena are due to a relaxation process leading to a lower energy state and that this process is closely related with magnetohydrodynamic (MHD) instabilities or fluctuations [9–15]. Primary interest in RFP physics concerns the causal mechanism of this relaxation process.

Measurement of the soft X-ray array is the most effective method of investigating the dynamic processes in the plasma and this method has been employed in tokamak [16, 17] and RFP experiments [5, 9, 18]. On the ZT-40M RFP, it is found that at relatively high Θ ($\Theta = B_p(a)/\bar{B}_t$), large amplitude sawtooth oscillations are largely correlated poloidally and toroidally [5, 9]. This soft X-ray activity is associated with simultaneous oscillations of the plasma current, toroidal flux, loop voltage, density and temperature as well as magnetic perturbations. It is also found that soft X-ray oscillations and magnetic perturbations become more intensive when Θ is increased. On the HBTX 1A RFP, no large scale sawtooth oscillations of the soft X-ray signal were observed [18]. However, in a high Θ discharge, a global mode with m = 0 and n = 0 was found when the soft X-ray and magnetic fluctuation signals were investigated with a statistical technique. This suggests that MHD mechanisms similar to those observed in ZT-40M are active even in cases without sawtooth oscillations. On ETA BETA II and

* Present address: Princeton Plasma Physics Laboratory, Princeton University, P.O. Box 451, Princeton, NJ 08544, USA.

REPUTE-1, it was found by internal magnetic measurements that relaxations of the magnetic configuration occurred periodically in the sustainment phase of the RFP plasma at relatively high Θ [10, 19, 20]. It has also been reported that a lower limit of the on-axis safety factor q(0) exists and that q(0) plays an important role in driving MHD instabilities, analogous to observations on tokamaks [21].

Numerical calculations with a three-dimensional non-linear MHD code [13, 15] suggest that the global development of the magnetic flux surfaces is caused by m = 1 internal kink modes and the non-linear m = 0 mode and that this leads to a relaxation process in the sustainment phase. However, the experimental results could not be explained self-consistently with these theories.

REPUTE-1 [22, 23] is an RFP device which has a resistive shell with a skin time of 1 ms; the plasma equilibrium can be controlled by external equilibrium field coils. Currently, it operates without limiters, with a plasma current in the range of 80–240 kA. For ramped current discharges, a duration of up to 3.2 ms is obtained, which corresponds to 3.2 times the skin time of the resistive shell.

In this paper, we present results of soft X-ray measurements on REPUTE-1. The X-ray system consists of seven and eleven surface barrier diodes (SBDs). It can view a minor cross-section of the plasma from both the vertical port and the horizontal diagnostic port. Applying a standard tomographic technique to the soft X-ray data [24], it is for the first time that we can reconstruct a two-dimensional image of the RFP plasma and study the phenomena occurring during RFP plasma relaxation. Magnetic perturbations are measured simultaneously by magnetic pick-up coils and toroidal flux loops. On the basis of these results, the dynamic mechanism of the relaxation process in the RFP plasma has been investigated experimentally.

The diagnostics used and their location around the torus are presented in Section 2. The parameters of the REPUTE-1 RFP discharge and the target plasma for the soft X-ray measurements are described in Section 3. Results of the soft X-ray tomography analysis are reported in Section 4. The toroidal propagation of the large amplitude oscillations of the soft X-ray signal is investigated by correlation analysis in Section 5. The magnetic fluctuations accompanying these oscillations are studied in Section 6. The results of our investigations of the soft X-ray and magnetic fluctuations in connection with the relaxation process of the RFP plasma are discussed in Section 7. Conclusions are presented in Section 8.

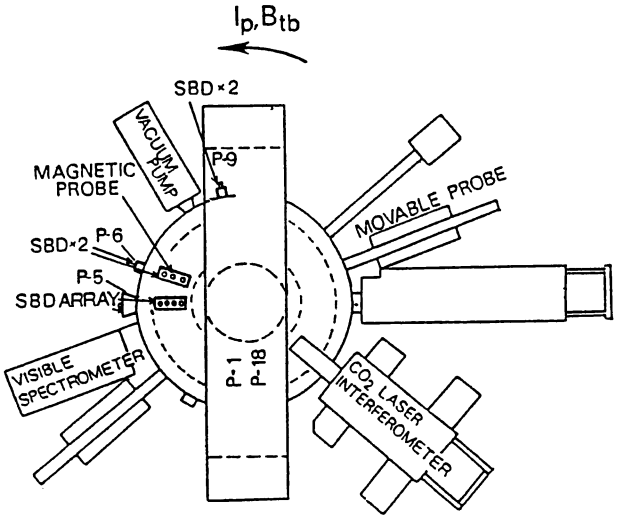

FIG. 1. Top view of the arrangement of diagnostics in REPUTE-1. Two sets of SBD arrays are located at the vertical and horizontal diagnostic ports P-5. Magnetic probes measuring the magnetic fluctuations at the plasma boundary are located at port P-6. The arrow indicates the direction of the plasma current I_p and the toroidal bias field B_{tb}.

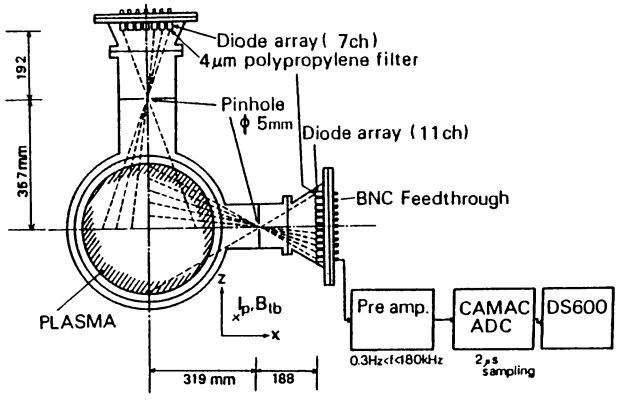

FIG. 2. Schematic view of SBD arrays: 7 SBDs are installed at the vertical port and 11 SBDs at the horizontal port. The soft X-rays emitted from the plasma are detected by each SBD array, passing through an imaging pinhole of 5 mm diameter. A 4 μm thick polypropylene foil filter is placed in front of the detector.

2. DIAGNOSTICS

The arrangement of the major diagnostic systems is shown in Fig. 1. Two sets of SBD arrays, located at port P-5, are used to investigate the time evolution of the soft X-ray emissivity profile. A schematic view of the SBD arrays is presented in Fig. 2. Arrays of seven

and eleven SBDs are arranged so that they can view a minor cross-section of the plasma from the vertical and horizontal diagnostic ports, respectively, at the same toroidal position. The SBD detectors are mounted on insulated BNC type feedthroughs so that they are electrically isolated from each other. The soft X-rays emitted from the plasma pass through a circular pinhole of 5 mm diameter and are imaged on each diode array. These arrays can view a cross-section of the plasma from x = −12.5 cm to x = +12.5 cm horizontally with a chord separation of about 4.1 cm, and from z = −17.0 cm to z = +17.0 cm vertically with a chord separation of about 3.4 cm.

The detector we used, ORTEC model RC-017-050-100, is a partially depleted SBD, which has an active detection area of 50 mm^2 and is covered with a 0.15 μm aluminium rectifying contact. In front of each detector, a 4 μm polypropylene foil filter is placed, and the Al rectifier and the foil filter modify the photon efficiency of the detector to eliminate unwanted visible and UV light. In the wavelength region where the instrument is sensitive, line radiation from light impurities such as oxygen or carbon ions is dominant. From previous spectroscopic measurements [18] it was reported that the photo-current of the diode is a monotonic function of the temperature and density (i.e. $n_e^2 T_e^\gamma$, where $\gamma = 4$) when it is dominated by light impurity emission such as from C V. In the electron temperature range of the REPUTE-1 experiment ($\gtrsim 150$ eV) [23], a dominant line radiation of C V (2271 Å) and a burnthrough of the line emission from the O V state (2781 Å), which has a lower ionization energy, have been observed by a visible spectrometer. Thus, we expect that the output current of the detector is proportional to $n_e^2 T_e^\gamma$, where $\gamma = 3.5$, assuming bremsstrahlung radiation from a pure hydrogen plasma. The preamplifier converts the electric current generated in the SBD detector to voltage, with a gain of 16 $V \cdot \mu A^{-1}$. A bias voltage of −36 V is applied to reduce the response time of the SBD detector. The frequency response of the detector and amplifier system extends from 0.3 Hz to 200 kHz. The output signal is sampled by the CAMAC system with a frequency of 500 kHz.

The line averaged soft X-ray data have been reconstructed to obtain the cross-sectional emissivity profile with a standard tomography technique [24]. The method used by us has been developed by Cormack [25]; it has the advantage of minimizing numerical errors by applying a least-squares fit with orthogonal expansion. The detector configuration on REPUTE-1 allows the X-ray emission to be reconstructed without having to make assumptions about the symmetry and rotation of the plasma. The X-ray emission is described by Zernicke polynomials of order m, ℓ, which determine the minor radial dependence, and by angular harmonics sin mθ and cos mθ. To concentrate on phenomena driven by the global MHD activity, m = 0, 1 and 2 angular components are considered and higher modes are ignored. Comparing the original raw chordal signals with the line averaged data of a reconstructed two-dimensional image, we conclude that this reconstruction describes the soft X-ray emissivity profiles with an error of 5%.

In addition to this SBD system, two sets of simple arrays are located at ports P-6 and P-9, which correspond to −20° and −80° in the toroidal direction, respectively (with the minus value indicating the antiparallel direction with respect to the plasma current I_p and the toroidal bias field B_{tb}). As shown in Fig. 3, each array consists of the same two SBDs with a 4 μm polypropylene filter and views $\pm$7.0 cm off-axis in the poloidal direction. The SBDs mainly measure poloidal m = 0 or 1 global fluctuations in the soft X-ray signals at different toroidal positions.

The high frequency component (f ≤ 250 kHz) of the magnetic fluctuations near the plasma boundary, $\dot{B}_{tw}$, $\dot{B}_{pw}$, is measured at port P-6 by three sets of magnetic probe coils, as shown in Fig. 3. Two toroidal flux loops are wound on the outside around the vacuum chamber at port P-8 (−60°) and at port P-17 (+120°). Since the skin time of the vacuum chamber

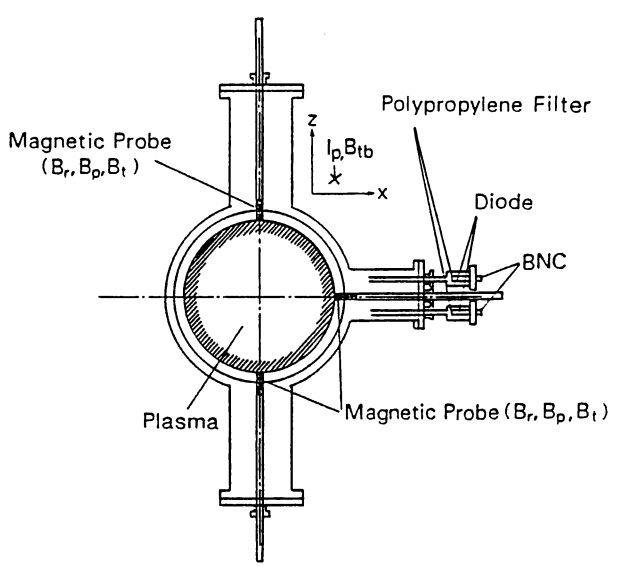

FIG. 3. Cross-sectional view of the additional SBD array at port P-6. Magnetic probes are inserted from the top, bottom and side ports and can measure the high frequency magnetic fluctuations.

for the toroidal magnetic field is 270 μs, it is difficult to observe the higher frequency component of the toroidal magnetic fluctuation.

The line averaged electron density is measured with a CO_2 laser interferometer at port P-16 (+140°). The minimum detectable density is 2×10^{18} m^{-3}.

3. PLASMA PARAMETERS

The REPUTE-1 experiment has been carried out with a plasma current in the range of 80 kA $\leq I_p \leq$ 240 kA [23]. With a constant value of the charging voltage of the capacitor bank to set up the Ohmic heating, the maximum value of I_p has a tendency to increase with the initially applied B_{tb}. The toroidal magnetic flux Φ_t contained in the plasma is proportional to I_p and is about 1.3×10^{-2} Wb for I_p = 200 kA. As I_p is increased, the discharge duration is also increased and the toroidal one-turn loop voltage V_ℓ is reduced. As regards the discharge duration, with ramped current operation of $\dot{I}_p$ = 80 kA·ms^{-1} the RFP plasma can be maintained by the external equilibrium field up to 3.2 ms. In this case, the plasma resistance R_p, defined as V_ℓ divided by I_p, is 30% higher than in flat-top and decay current operations. The filling gas pressure P_f is controlled by piezoelectric valves, and typical values of P_f range from 1.0 to 5.0 mtorr. The line averaged electron density $\bar{n}_e(0)$ is approximately proportional to P_f during the discharge.

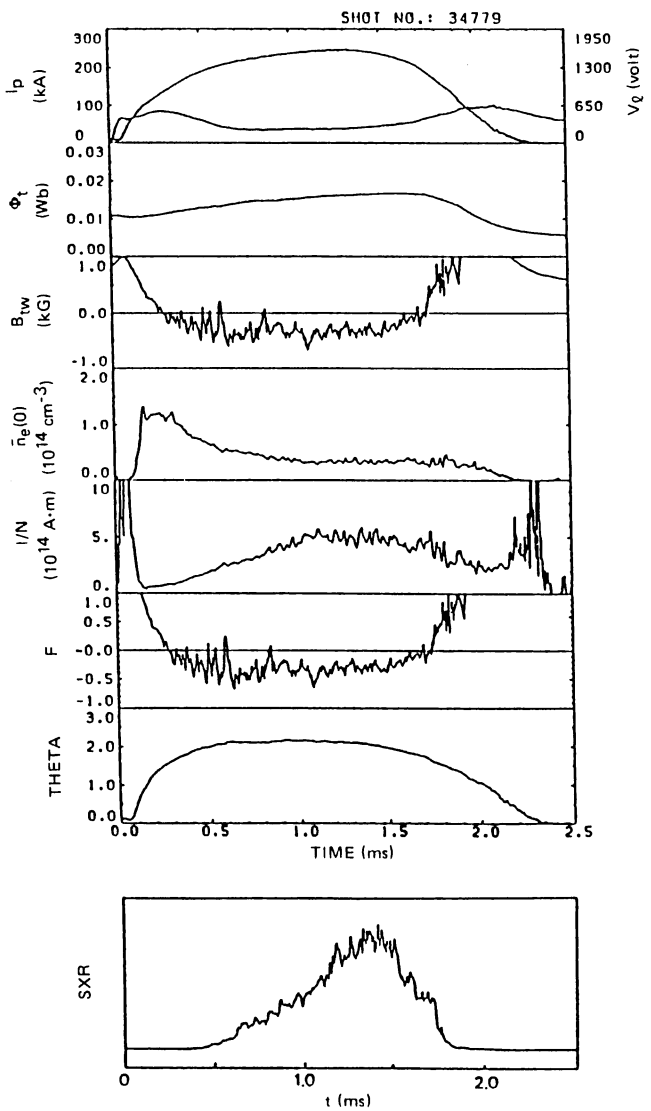

FIG. 4. Time evolution of the plasma parameters for the high I/N discharge. Plasma current I_p, loop voltage $\bar{V}_\ell$, toroidal magnetic flux Φ_t, toroidal magnetic field at the wall B_{tw}, line averaged electron density $\bar{n}_e(0)$, field reversal ratio F, pinch parameter Θ, and soft X-ray signal.

The soft X-ray signal increases if I_p is increased and at the same time $\bar{n}_e(0)$ is decreased, i.e. I/N is increased (I corresponds to I_p and N corresponds to the averaged electron density within the poloidal cross-section $\pi a^2 \bar{n}_e(0)$). In particular, when I/N exceeds $\sim 5.0 \times 10^{-14}$ A·m, which is achieved by operation at high I_p ($\geq$200 kA) and low P_f ($\leq$1.6 mtorr), a strong soft X-ray signal is observed. Figure 4 presents the typical time evolution of the plasma parameters and the line of sight of the soft X-ray emission. The fluctuation amplitude $\tilde{I}_{sx}/I_{sx}$ grows by more than 20% and the X-ray signals are well correlated across the plasma core region. When the RFP plasma is sustained for a relatively long period (more than 2.0 ms), Θ remains large ($2.1 \leq \Theta \leq 2.3$) and $F = B_t(a)/\bar{B}_t$ oscillates in the range of $-0.3 \geq F \geq -0.5$. In Section 4, we investigate the results obtained from the target plasma which is sustained in the high I/N regime with strong soft X-ray signals, as shown in Fig. 4.

4. TOMOGRAPHY RESULTS

Figure 5 shows the time evolution of the soft X-ray signals over the period t = 1.0–1.4 ms, for the discharge shown in Fig. 4 (enlarged). The vertical broken lines show the times when the soft X-ray signal becomes peaked in the plasma centre (x = z = 0). Discrete events appear periodically both in the soft X-ray signal and in the $\dot{\Phi}_t$ signal. At each event, the soft X-ray emissivity rises to its maximum associated with small amplitude oscillations ($\Delta I_{sx}/I_{sx} \leq 10\%$). Following the peaking of the signal, a large crash can be observed in the hot core region. Here, we call the

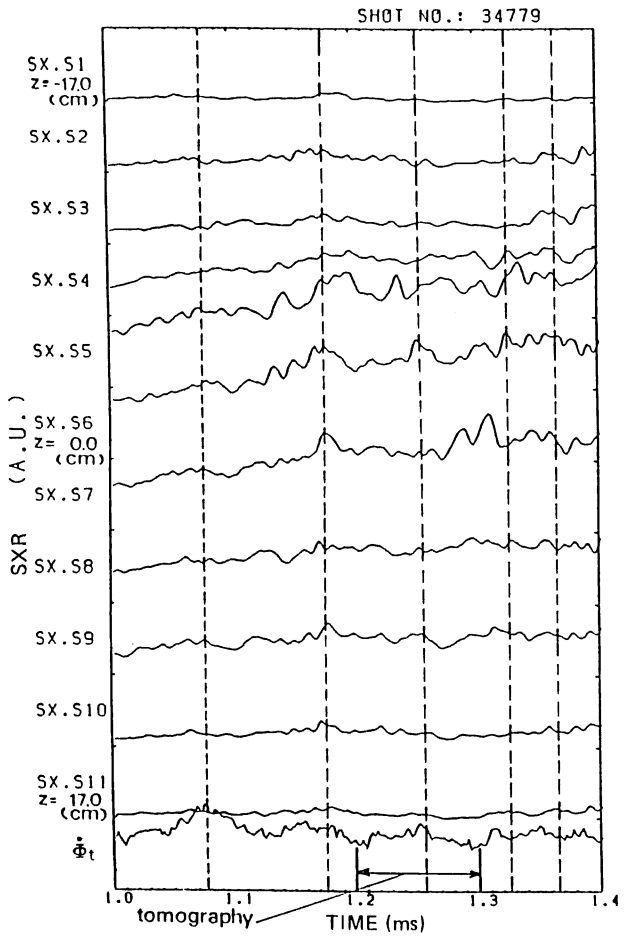

FIG. 5. Time evolution of the soft X-ray signals measured by the SBD array installed at the horizontal port, over the period t = 1.0–1.4 ms. This is the same discharge as that shown in Fig. 4. The vertical broken lines indicate the times when the soft X-ray emissivity becomes peaked in the plasma centre (x = z = 0).

weak oscillation the 'precursor oscillation' and the period between two large crashes the 'event period'. The event period ranges from 60 to 150 μs and has a tendency to become shorter as the plasma current is increased.

Figures 6 and 7 illustrate the soft X-ray emissivity profiles and contours for the event shown in Fig. 5. These drawings have been reconstructed from tomographic measurements. The period t = 1.23–1.25 ms corresponds to that of one precursor oscillation. The plasma hot core moves from the centre of the line to the lower left, as shown in Fig. 7. The displacement is relatively small ($\Delta r/a \leq 15\%$) and a slight m = 1 deformation of the emissivity contour can be observed.

When the plasma hot core is displaced, the emissivity of the hot core decreases ($\Delta I_{sx}/I_{sx} \leq 10\%$), as shown in Fig. 6.

After the precursor oscillation, the emissivity profile becomes strongly peaked at t ~ 1.25 ms. During this peaking, the displacement of the plasma hot core is small and the emissivity contour is almost axisymmetric. At t = 1.27 ms, a large crash of the emissivity profile begins. The drop in soft X-ray emissivity $\Delta I_{sx}/I_{sx}$ is more than 20%. The duration of the large crash is always about 30 μs (corresponding to 100 × τ_A in the REPUTE-1 experiments). Figure 8 shows an expanded time evolution of the soft X-ray emissivity contours during the large crash. The displacement of the hot core is increased ($\Delta r/a \geq 20\%$) and the emissivity contours are distorted by the m = 1 mode. In the period t = 1.280–1.286 ms, the emissivity profile changes to a hollow one (the dark areas in Fig. 8 are for the same emissivity contours).

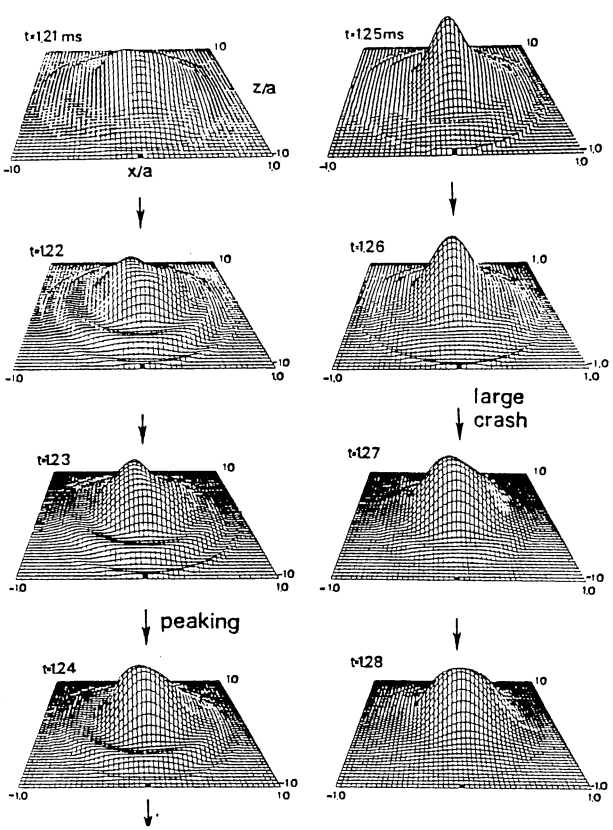

FIG. 6. Soft X-ray emissivity profiles over the period t = 1.21–1.28 ms. The emissivity in the hot core region increases rapidly from 1.24 to 1.26 ms. Subsequently, a large crash starts at 1.26 ms.

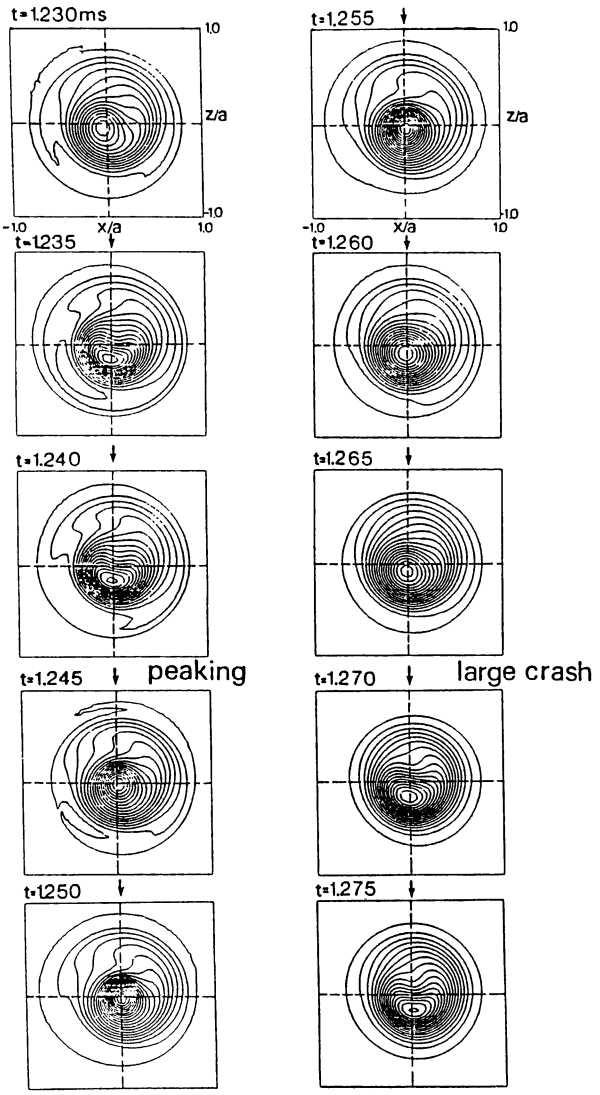

FIG. 7. Contours of the soft X-ray emissivity for one event, corresponding to the profiles shown in Fig. 6.

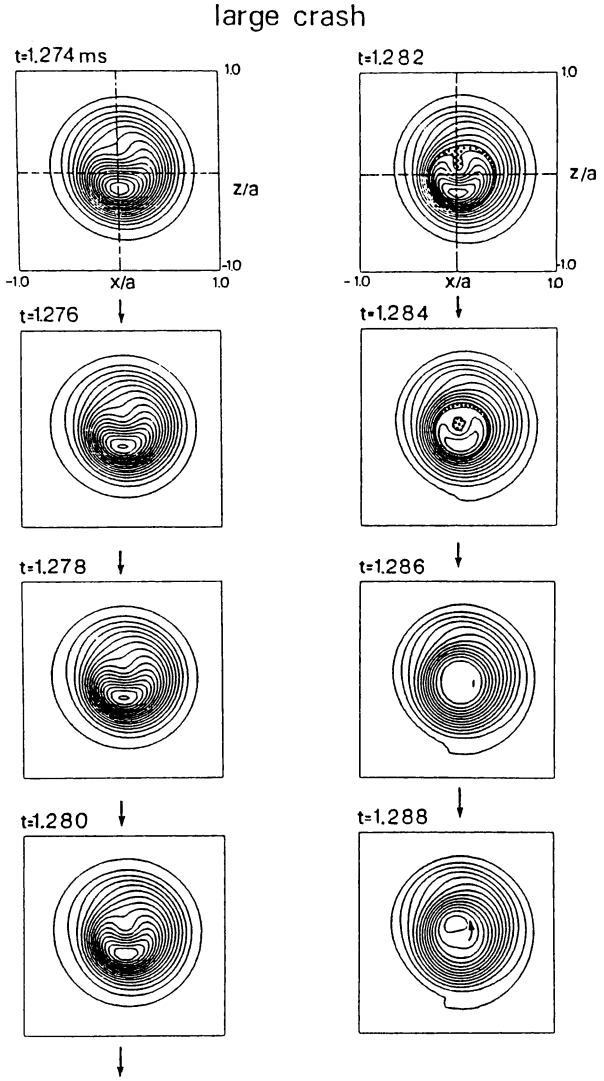

FIG. 8. Contours of the soft X-ray emissivity during the large crash process from 1.274 to 1.288 ms. The contours become m = 1 distorted and the displacement of the hot core increases. A hollow profile appears in the period 1.282–1.284 ms. The hot core starts to rotate counter-clockwise from 1.284 to 1.296 ms.

It should be noted that, although a remarkable m = 1 distortion is generally observed during the large crash, a hollow emissivity profile does not always appear to be present. Following this distortion, after t = 1.284 ms, a rotation of the plasma hot core in the ion diamagnetic direction (counter-clockwise, Fig. 8) is observed. Consequently, the soft X-ray emissivity profile, exhibiting periodical peaking and succeeding large crashes across the entire plasma cross-section, qualitatively illustrates the evolution of the real plasma shape under the influence of the rapid changes of the temperature and density profiles during the relaxation period.

For a detailed interpretation, the source of the soft X-ray emission has to be considered. Assuming that the soft X-ray is emitted from the plasma as a result of bremsstrahlung or recombination radiation, the emissivity contours shown in Fig. 8 could be used to describe the real reconnection of the magnetic flux surfaces, since the continuum radiation is well expressed as a function of T_e, n_e and Z_{eff} [26]. If, instead, the X-ray emissivity is dominated by impurity line radiation, which is described in Section 2, then we have a relatively qualitative picture of the real plasma shape.

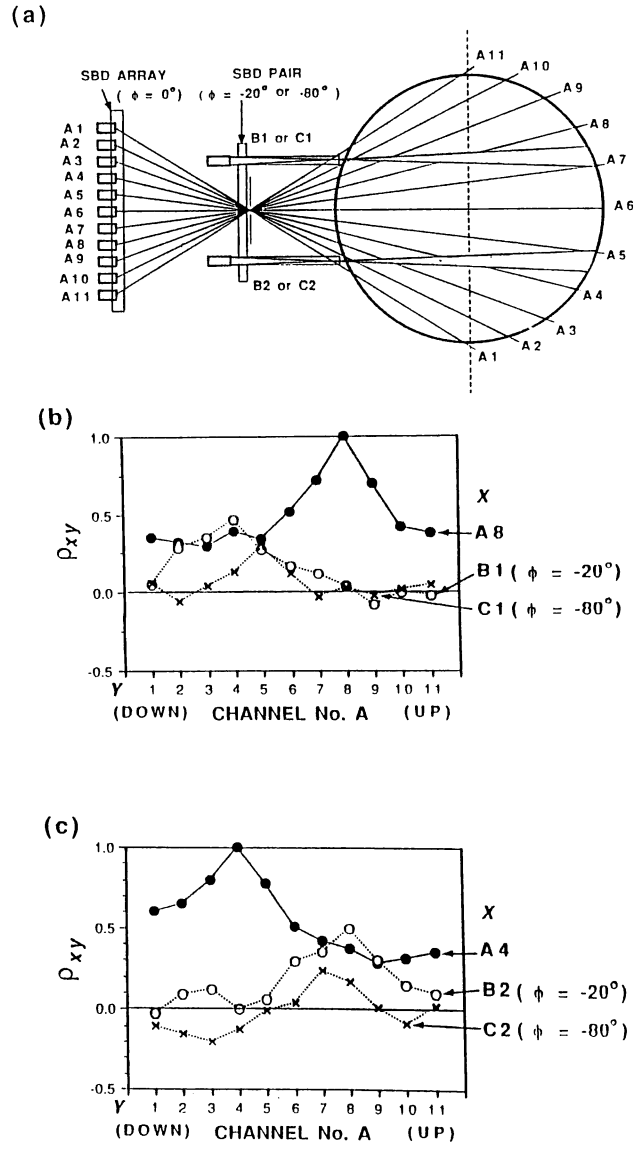

FIG. 9. (a) Schematic diagram of the sight-lines of the main SBD array and the additional SBD arrays installed at the vertical ports P-6 and P-9 (-20° and -80° in toroidal angle, respectively). Normalized covariance, $\rho_{xy} \equiv R_{xy}(0)/\sqrt{R_{xx}(0)R_{yy}(0)}$, between a detector x and a detector y.
(b) ρ_{xy} versus Y for the A8, B1 and C1 detectors (along the upper sight-line).
(c) ρ_{xy} versus Y for the A4, B2 and C2 detectors (along the lower sight-line).

5. TOROIDAL PROPAGATION

The toroidal propagation of the large amplitude oscillations in the soft X-ray signals is investigated by correlation analysis of toroidally separated SBD signals. Figure 9(a) is a schematic diagram of the sight-lines of the main SBD array and of the additional SBD arrays installed at the vertical ports P-6 and P-9 (-20° and -80° in toroidal angle, respectively). The chord radius of the sight-line of the B1 (or C1) detector on the P-6 (or P-9) SBD array is the same as that of the A8 detector on the main array, and the difference of the two chord angles is 23° in the poloidal direction. Since most of the X-rays are emitted from the hottest and densest part of the plasma, the main part of the emission measured with the B1 or C1 detector (B2 or C2 detector) in each minor cross-section is approximated by that measured with the A8 detector (A4 detector).

To obtain some information about the toroidal propagation, we have used statistical techniques. The correlation function is defined as

$$R_{xy}(\tau) = \left\langle \int_{t_0}^{t_0+T} x(t+\tau)\, y(t)\, dt \right\rangle \qquad (1)$$

where x and y are signals from a pair of detectors. $R_{xy}(\tau)$ is calculated by averaging over a few consecutive discharges in a time interval of 1.0–1.5 ms, during which global activity in soft X-ray emission is periodically observed. For the investigation of the frequency band of 5–100 kHz, the digital signals are filtered. This frequency range includes the event period of the global activity described by the tomography analysis (Section 4). Above about 100 kHz, the fluctuation has a shorter cross-field correlation length, and no toroidal correlation between the signals measured by the toroidally separated detectors (A8 and B1) is observed. The higher frequency fluctuation is considered to be a 'local turbulence' as observed in HBTX 1A [18] and no cross-field correlation has been found.

Figures 9(b) and (c) represent the normalized covariance, $\rho_{xy} \equiv R_{xy}(0)/\sqrt{R_{xx}(0)R_{yy}(0)}$, between a detector x and a detector y (one of those in the main SBD array). The solid line in Fig. 9(b) (or Fig. 9(c)) shows ρ_{xy} between the A8 detector (or A4) and the other detectors in the main array. Since the correlation is positive across the entire minor cross-section, the global activity has a long cross-field correlation, and an even poloidal mode such as m = 0 dominates rather than an odd mode such as m = 1. The dotted lines show ρ_{xy} between one of the detectors on the additional SBD array and the detectors in the main SBD array. Again, the values of ρ_{xy} are positive across a wide minor radius, which is evidence of the m = 0 mode. Compared with ρ_{xy} of the A8 detector (solid line in Fig. 9(b)), the signal of the B1 detector is well

correlated with the signals of the detectors adjacent to A4, which views the plasma along the lower off-axis path across the minor cross-section. On the contrary, ρ_{xy} of the B2 detector (Fig. 9(c)) shows good correlation with the detectors adjacent to A8 with an upper off-axis sight-line. The correlation between the C1 (or C2) detector and the detectors in the main SBD array is poor; the negative correlation between opposite detectors with respect to the plasma centre indicates that an odd poloidal mode may exist there. From these results, we conclude that the global activity in soft X-ray emission has at least two poloidal modes. The first is predominantly an even mode such as m = 0, the correlation length of which ranges from 20° to 80° in the toroidal direction. The second is an odd mode such as m = 1, with a smaller amplitude. Since the correlation between the detectors displaced by 20° in the toroidal direction indicates that peaking occurs at nearly opposite positions with respect to the midplane, this mode has a relatively high toroidal number such as n ~ 9.

6. MAGNETIC FLUCTUATIONS

We have measured the magnetic fluctuations in the toroidal and poloidal directions at the plasma boundary with the magnetic probe coils located at the same toroidal position (P-6) as one of the detectors in the additional SBD array. The power spectrum of the magnetic fluctuations during the active soft X-ray period, t = 1.0–1.5 ms, is relatively broad, without a significant peak above 10 kHz. The correlation function $R_{xy}(\tau)$, given by Eq. (1), is used for determining the structure of the fluctuation. Here, x and y are the magnetic probe signals $\dot{B}_{tw}$ (or $\dot{B}_{pw}$) in the toroidal (or poloidal) direction. $R_{xy}(\tau)$ is measured by averaging over the same five consecutive shots and over the same time period as in Section 5. Each signal is filtered to obtain a frequency of 5–50 kHz for the low frequency fluctuations or 50–200 kHz for the high frequency fluctuation.

The correlation functions $R_{xy}(\tau)$ of the toroidal magnetic fluctuation for the low and high frequency bands are shown in Figs 10(a) and (b). $R_{xy}(\tau)$ of the low frequency fluctuation is positive at a time lag of $\tau = 0$ and negative at $\tau \sim -50$ or $+30$ μs. The low frequency fluctuation is predominantly caused by an even mode such as m = 0. In contrast, $R_{xy}(\tau)$ of the high frequency fluctuation is negative at $\tau = 0$ and clearly positive in a narrow region around $\tau \sim 0$. This result indicates that the high frequency fluctuation has an odd

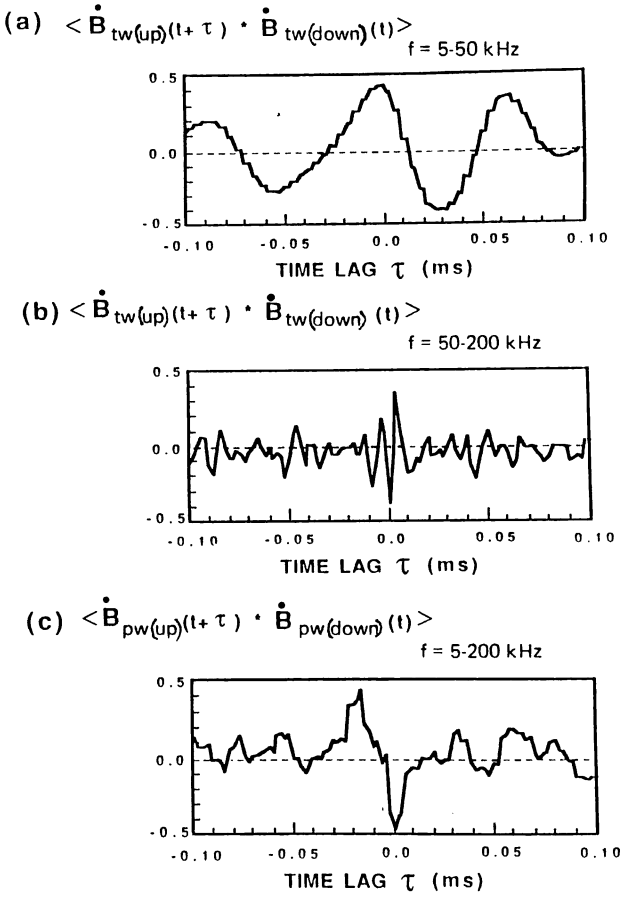

FIG. 10. Correlation functions $R_{xy}(\tau)$ of the magnetic fluctuations (a) for low frequency (5–50 kHz) $\dot{B}_t$; (b) for high frequency (50–200 kHz) $\dot{B}_t$; (c) for $\dot{B}_p$ of f = 5–200 kHz.

mode such as m = 1. Figure 10(c) shows $R_{xy}(\tau)$ of the poloidal magnetic fluctuation for the entire frequency band of f = 5–200 kHz, which has a negative correlation at $\tau = 0$ and a positive correlation at $\tau \sim -20$ μs. It is found that the poloidal magnetic fluctuation is predominantly caused by an odd mode such as m = 1 and propagates from top to bottom along the plasma surface with a velocity $v_p = 35$ km·s^{-1}.

Figure 11 shows the time evolution of the line-of-sight signals of the additional SBD array installed at port P-6 and the magnetic fluctuation signals $\dot{B}_{tw}$ and $\dot{B}_{pw}$ at the same port. Also shown is $\dot{\Phi}_t$ measured at ports P-8 and P-17 (-60° and +120° in the toroidal direction, respectively). This is the same shot as that presented in Fig. 5. Here, the soft X-ray signals are filtered to remove the 'local turbulence' fluctuation with a frequency above 100 kHz. $\dot{\Phi}_t$ is also filtered to eliminate the frequency fluctuation above 100 kHz

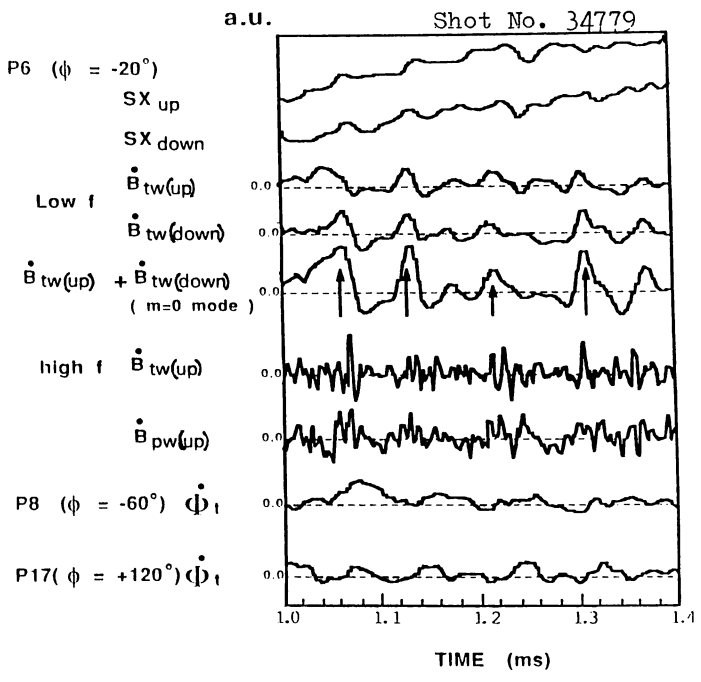

FIG. 11. Time evolution of SX_{up} and SX_{down} for line-of-sight signals of the additional SBD array installed at port P-6. $\dot{B}_{tw(up)}$ and $\dot{B}_{tw(down)}$ for the low frequency (5–50 kHz) toroidal magnetic fluctuation; sum of $\dot{B}_{tw(up)} + \dot{B}_{tw(down)}$ describing m = 0 activity; $\dot{B}_{tw(up)}$ for high frequency (50–200 kHz) m = 1 fluctuation; $\dot{B}_{pw(up)}$ for the entire frequency band (5–200 kHz) of the poloidal fluctuation; $\dot{\Phi}_t$ for the toroidal flux fluctuation measured at ports P-8 and P-17.

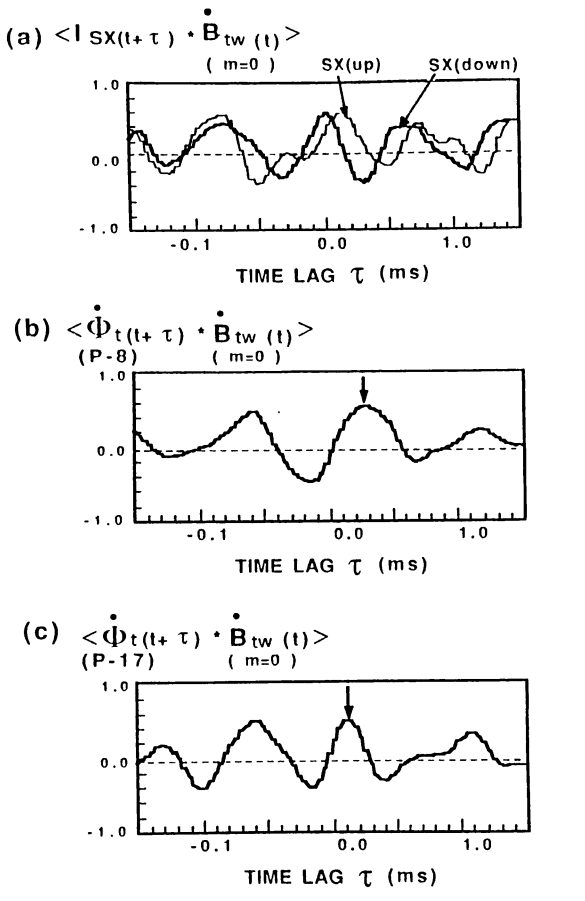

FIG. 12. Correlation function $R_{xy}(\tau)$: (a) for the soft X-ray signals and for $\dot{B}_{tw(up)} + \dot{B}_{tw(down)}$ shown in Fig. 11, (b) $\dot{\Phi}_t$ at port P-8 and (c) $\dot{\Phi}_t$ at port P-17 and $\dot{B}_{tw(up)} + \dot{B}_{tw(down)}$.

because it contributes little to the toroidal flux generation. The toroidal magnetic fluctuation $\dot{B}_{tw}$ for the low frequency band (f = 5–50 kHz) and the high frequency band (f = 50–200 kHz) are illustrated separately. Also shown is the time evolution of $\dot{B}_{tw(up)} + \dot{B}_{tw(down)}$ illustrating the growth of the even mode (mainly m = 0). The arrows indicate the time when this mode grows. It is found that the amplitude of the high frequency fluctuation of the toroidal magnetic field rises simultaneously. In contrast to the toroidal magnetic fluctuation, the m = 1 poloidal fluctuation remains large and grows somewhat.

Figure 12(a) presents the correlation function $R_{xy}(\tau)$ for the soft X-ray signals and for $\dot{B}_{tw(up)} + \dot{B}_{tw(down)}$, where both signals are filtered to obtain the frequency band 5–50 kHz. Since the two signals are well correlated for a zero time lag, we find that the growth of the m = 0 mode (and also the m = 1 mode) in the toroidal magnetic fluctuation coincides with the peaking of the soft X-ray emissivity.

Figures 12(b) and (c) present the correlations between $\dot{B}_{tw(up)} + \dot{B}_{tw(down)}$ and the fluctuation signal of the toroidal flux loop, $\dot{\Phi}_t$, shown in Fig. 11. The correlation functions of $\dot{\Phi}_t$ measured at ports P-8 and P-17 are positive at a time lag of τ = +10 and +25 μs, respectively. Since these time lags are relatively small and positive with respect to the interval of the event ($\sim$ 100 μs), it is found that m = 0 toroidal magnetic fluctuations contribute to the toroidal flux generation.

7. SUMMARY AND DISCUSSION

In this section, we discuss the relaxation phenomena of the RFP plasma in the sustainment phase. The results of the soft X-ray measurements are summarized in Section 7.1. The plasma configurations during the relaxation phase are compared with numerical results of an MHD stability calculation for the m = 1 kink modes in Section 7.2.

7.1. Soft X-ray measurements

The peaking of the soft X-ray emissivity profile and the succeeding large crash have been described by tomography analysis (Section 4). Before the large crash of the soft X-ray profile, a small precursor oscillation has been observed which has an m = 1 character and a period of ~20 μs. Similar m = 1 precursors have been observed on ZT-40M [7] with a one-dimensional SBD array. It is reported in Ref. [7] that the activity is localized within the inside half of the minor cross-section (in particular, it is dominant at the off-axis chord); this is explained in Ref. [12] as a resistive tearing mode. Note that the precursor oscillation measured in our experiment is localized within a narrower central region (displacement of the hot core, r/a ~ 15%) and that it is also observed in the plasma centre. This could still be explained by an eigenfunction caused by the resistive tearing mode.

During the large crash of the soft X-ray emissivity profile, which starts just after the axisymmetric peaking of the profile (Fig. 8), the m = 1 deformation increases (see Section 4). Using correlation analysis, we have found that the global activity has at least two different modes. One is the mode predominantly caused by axisymmetry across the minor cross-section, the correlation length of which ranges from 20° to 80° in the toroidal direction. The other is the smaller m = 1 mode with a high toroidal mode number (n ~ 9).

Soft X-ray measurements have been performed in ZT-40M [5] and HBTX 1A [18]; it is found that the X-rays are associated with a relaxation of the RFP plasma. In particular, at high Θ operation, the soft X-rays have a different form in the two cases (the fluctuation is called 'sawtooth' in ZT-40M and 'breathing' of the plasma column in HBTX 1A). However, the two kinds of fluctuation have some similarities such as a long toroidal correlation length of the m = n = 0 mode, the existence of an inversion radius and a good correlation with magnetic activity. In the REPUTE-1 experiment, the short toroidal correlation length of the axisymmetric mode presumably reflects the fact that the classical electron diffusivity and the thermal conductivity parallel to B are not so good that the magnetic field lines can be considered isothermal and isobaric, because of a relatively high plasma resistivity. The existence of an inversion radius has not been observed. The crash period is about 30 μs, which corresponds to 100 $\times$ τ_A, and this time-scale is similar to that measured in ZT-40M.

The fluctuation of the soft X-ray signals is associated with a growth of the toroidal magnetic fluctuation, which has an m = 0 mode for the low frequency regime and an m = 1 mode for the high frequency regime, while the poloidal magnetic fluctuation is predominantly caused by an m = 1 mode for the entire frequency band. The strength of the magnetic fluctuation in the sustainment phase of the high Θ discharge is generally similar to that observed in other RFP experiments [5, 31]. The fluctuation of the toroidal magnetic flux $\dot{\Phi}_t$ rises above zero simultaneously with the growth of the m = 0 magnetic fluctuations. The m = 0 toroidal magnetic fluctuations are especially important because they contribute to the toroidal flux generation, which is produced by the relaxation of the RFP plasma and plays an essential role in sustaining the RFP configuration.

7.2. Relaxation phase

We discuss here our stability diagram, with the relation between the field reversal ratio F and the fluctuation of the toroidal magnetic flux $\dot{\Phi}_t$, $F \equiv B_t(a)/(\Phi_t/\pi a^2)$. The average of the toroidal magnetic field on the plasma boundary, $B_t(a)$, measured experimentally, is expressed as

$$B_t(a) = -\frac{1}{2\pi R}\left\{NI_t + \frac{\dot{\Phi}_t}{R_\ell}\right\}$$

where N is the total turns of the toroidal coil, I_t is the toroidal coil current and R_ℓ is the liner resistance in the poloidal direction. The first and second terms on the right hand side of the equation correspond to the total toroidal coil current and the induced liner current in the poloidal direction. The fluctuations of $B_t(a)$ and F shown in Fig. 4 depend mainly on $\dot{\Phi}_t$, and the decrease of F to a more negative value in the fluctuation period indicates the increase of $\dot{\Phi}_t$ on the positive side (i.e. toroidal flux generation).

Various models of the RFP configuration and its stability to MHD modes have been discussed and these studies are reviewed in Ref. [27]. Recently, a simple model, in which $\mu(r) \equiv \mu_0\vec{j}\cdot\vec{B}/B^2$ is given by $(2\Theta_0/a) \times [1 - (r/a)^n]$, has been introduced and stability diagrams for m = 1 kink modes have been presented [28]. Here, Θ_0 and n are independent free parameters which can change the equilibrium configuration in a wide range of F and Θ values. Note that the local parameter Θ_0 corresponds to the on-axis value of the safety factor, $q(0) = a/(\Theta_0 R)$, and that it is essentially related to

the on-axis current density ($\Theta_0 = \mu_0 aj(0)/2B(0)$). The plasma configuration of this model with a high value of n approaches the Bessel Function Model (i.e. the force-free configuration).

We discuss the stability of the RFP field configuration in the sustainment phase using the MHD stability results given in Ref. [29]. We solve the dynamic equation of Hain and Lust [30] for the equilibrium configuration obtained by the following first-order differential equations

$$\frac{d\tilde{B}_t}{d\tilde{r}} = -2\Theta_0\tilde{\mu}\tilde{B}_p - \frac{\beta_{ax}}{2}\frac{\partial\tilde{p}}{\partial\tilde{r}}\frac{\tilde{B}_t}{\tilde{B}^2}$$

$$\frac{1}{\tilde{r}}\frac{d(\tilde{r}\tilde{B}_p)}{d\tilde{r}} = 2\Theta_0\tilde{\mu}\tilde{B}_t - \frac{\beta_{ax}}{2}\frac{\partial\tilde{p}}{\partial\tilde{r}}\frac{\tilde{B}_p}{\tilde{B}^2}$$

where $\tilde{r} = r/a$, $\tilde{\mu} = \mu/\mu(0)$, $\tilde{p} = p/p(0)$, $\tilde{B} = B/B_t(0)$ and $\beta_{ax} = 2\mu_0 p(0)/B^2(0)$. The minor radius of the conducting wall a_w is assumed to be 1.1 times the plasma minor radius a, which corresponds to that of REPUTE-1 ($a_w/a = 25/22$ cm).

Figure 13 illustrates the stability diagram for ideal internal m = 1 kink modes; n is varied from 2 to 6 for each q_0 value and the plasma pressure is assumed to be constant (corresponding to $\beta_{ax} = 5\%$) across the plasma minor cross-section. It is found that the stable region is above the solid line (i.e. marginal configuration for m = 1 internal kink modes). The experimental F and Θ values in the sustainment phase of the high Θ discharge are presented by the arrow 'a'. These are the typical values obtained in the soft X-ray measurement, as shown in Fig. 4. The experimental Θ and Θ_0 values obtained by using an internal probe array [20] in a low Θ discharge are indicated by the arrow 'b'. The diagram shows that when the soft X-ray emissivity profile becomes peaked, the measured F and Θ move to the right end of the arrow. In this area, the plasma configuration remains in the unstable region before relaxation. During relaxation of the soft X-ray emissivity, the F and Θ values move in the direction of the arrow 'a' in which the plasma configuration is more stable according to numerical results.

The same behaviour of the Θ and Θ_0 values is also found by internal probe measurements. Note that in the sustainment period of REPUTE-1 the F value extends to the relaxed state ($\Delta F \sim 0.2$) more than the Θ value ($\Delta\Theta \sim 0.1$) and that this fluctuation of the F value is mainly related to $\dot{\Phi}_t$. The growth of the m = 0 and m = 1 activity in the toroidal magnetic fluctuation is evidently correlated with this relaxation. Also, it is found that the relaxation of the soft X-ray emissivity

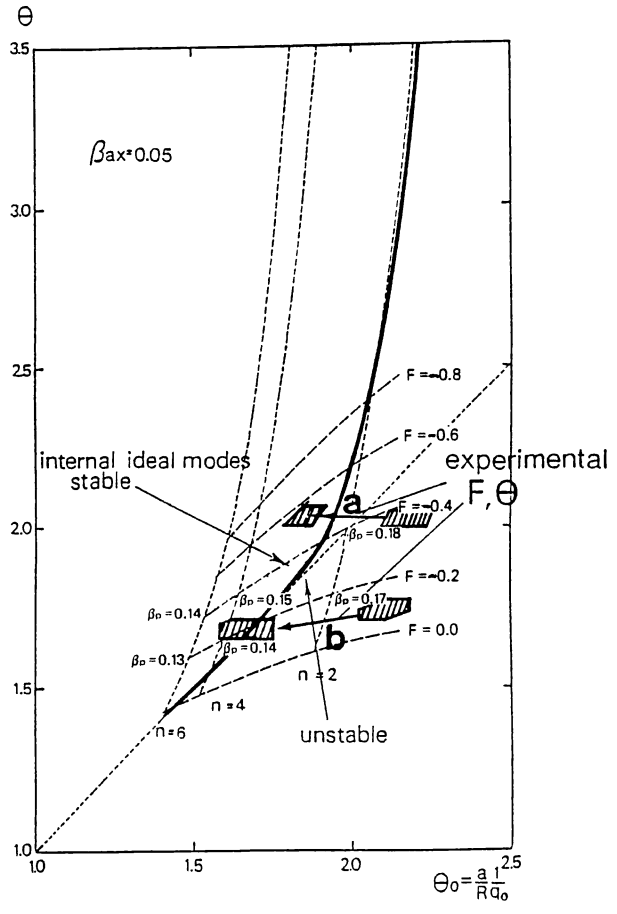

FIG. 13. Marginal Θ-Θ_0 diagram for m = 1 internal ideal MHD modes. The solid line indicates the internal ideal MHD marginal curve [29].
(a) Experimental results for F and Θ in the high Θ discharge shown in Fig. 4. (b) Internal probe results for Θ and Θ_0 in a low Θ discharge [20]. During the relaxation the field configurations move from an unstable region to a stable one.

profile obtained from an analysis of the tomographic measurements corresponds to a relaxation from a magnetic configuration unstable with respect to the m = 1 internal kink modes to a stable configuration.

8. CONCLUSIONS

In the sustainment phase of an RFP discharge, a characteristic fluctuation of the soft X-ray emissivity is seen. There is a peaking and a subsequent large crash of the emissivity profile after a few precursor oscillations. One period of the soft X-ray fluctuation ranges from 60 to 150 μs. The amplitude of the soft X-ray

fluctuation increases and the period becomes shorter as the plasma current increases during the same discharge, whereas the duration of the large crash is always about 30 μs (corresponding to 100 $\times$ t_A in the REPUTE-1 experiment). This soft X-ray activity has at least two modes: one is predominantly caused by an m = 0 mode, which corresponds to an axisymmetric increase or decrease of the soft X-ray emissivity profile, and the other is due to the m = 1 mode. The toroidal correlation length of the dominant m = 0 mode ranges from 20° to 80°, while the m = 1 mode has a high toroidal mode number (n ~ 9). In this crash process, a specific distortion of the emissivity profile can be observed. This indicates in a qualitative way the evolution of the plasma shape during relaxation. In contrast to the poloidal magnetic fluctuation which is predominantly caused by an m = 1 mode, the toroidal magnetic fluctuation has m = 0 and m = 1 modes, and the growth of the fluctuation amplitude is well correlated with the relaxation of the soft X-ray emissivity profile. We find that the soft X-ray fluctuations observed in our experiments reflect the relaxation mechanism of an RFP plasma. These phenomena are considered to be caused by global MHD activity.

REFERENCES

[1] BAKER, D.A., BAUSMAN, M.D., BUCHENAUER, C.J., et al., in Plasma Physics and Controlled Nuclear Fusion Research 1982 (Proc. 9th Int. Conf. Baltimore, 1982), Vol. 1, IAEA, Vienna (1983) 587.

[2] BODIN, H.A.B., BUNTING, C.A., CAROLAN, P.G., et al., ibid., p. 641.

[3] TAMANO, T., CARLSTROM, T., CHU, C., et al., ibid., p. 609.

[4] ANTONI, V., BAGATIN, M., BUFFA, A., et al., ibid., p. 619.

[5] WATT, R.G., NEBEL, R.A., Phys. Fluids **26** (1983) 1168.

[6] WERLEY, K.A., NEBEL, R.A., WURDEN, G.A., Phys. Fluids **28** (1985) 1450.

[7] HOWELL, R.B., INGRAHAM, J.C., WURDEN, G.A., WEBER, P.G., BUCHENAUER, C.J., Phys. Fluids **30** (1987) 1828.

[8] MOFFATT, H.K., Magnetic Field Generation in Electrically Conducting Fluids, Cambridge Univ. Press (1978).

[9] WURDEN, G.A., Phys. Fluids **27** (1984) 551.

[10] ANTONI, V., ORTOLANI, S., Phys. Fluids **30** (1987) 1489.

[11] HIRANO, Y., KONDOH, Y., MAEJIMA, Y., et al., in Plasma Physics and Controlled Nuclear Fusion Research 1984 (Proc. 10th Int. Conf. London, 1984), Vol. 2, IAEA, Vienna (1985) 475.

[12] CARAMANA, E.J., NEBEL, R.A., SCHNACK, D.D., Phys. Fluids **26** (1983) 1305.

[13] SCHNACK, D.D., CARAMANA, E.J., NEBEL, R.A., Phys. Fluids **28** (1985) 321.

[14] KUSANO, K., SATO, T., Nucl. Fusion **26** (1986) 1051.

[15] KUSANO, K., SATO, T., Nucl. Fusion **27** (1987) 821.

[16] VON GOELER, S., STODIEK, W., SAUTHOFF, N., Phys. Rev. Lett. **33** (1975) 1201.

[17] GRANETZ, R.S., SMEULDERS, P., Nucl. Fusion **28** (1988) 457.

[18] MALACARNE, M., HUTCHINSON, I.H., Plasma Phys. Controll. Fusion **28** (1986) 823.

[19] ANTONI, V., MARTIN, P., ORTOLANI, S., Plasma Phys. Controll. Fusion **29** (1987) 279.

[20] UEDA, Y., ASAKURA, N., MATUZUKA, S., et al., Nucl. Fusion **27** (1987) 1453.

[21] KADOMTSEV, B.B., in Plasma Physics and Controlled Nuclear Fusion Research 1976 (Proc. 6th Int. Conf. Berchtesgaden, 1976), Vol. 1, IAEA, Vienna (1977) 555.

[22] ASAKURA, N., FUJITA, T., HATTORI, K., et al., Plasma Phys. Controll. Fusion **28** (1986) 805.

[23] ASAKURA, N., FUJISAWA, A., FUJITA, T., et al., in Plasma Physics and Controlled Nuclear Fusion Research 1986 (Proc. 11th Int. Conf. Kyoto, 1986), Vol. 2, IAEA, Vienna (1987) 449.

[24] TSUJI, S., NAGAYAMA, Y., KAWAHATA, K., NODA, N., TANAHASHI, S., Nucl. Fusion **22** (1982) 1082.

[25] CORMACK, A.M., J. Appl. Phys. **24** (1985) 787.

[26] De MICHELIS, C., MATTIOLI, M., Nucl. Fusion **21** (1981) 677.

[27] BODIN, H.A.B., NEWTON, A.A., Nucl. Fusion **20** (1980) 1255.

[28] ANTONI, V., MERLIN, D., ORTOLANI, S., PACCAGNELLA, R., Nucl. Fusion **26** (1986) 1711.

[29] FUJISAWA, A., ONODERA, S., MIYAMOTO, K., "Ideal MHD instabilities with finite beta effect in a reversed field pinch", to be published in J. Phys. Soc. Jpn.

[30] HAIN, K., LUST, R., Z. Naturforsch. **13a** (1958) 936.

[31] HUTCHINSON, I.H., MALACARNE, M., NOONAN, P., Nucl. Fusion **24** (1984) 59.

(Manuscript received 16 May 1988
Final manuscript received 28 March 1989)